An Adaptive Kalman Fusion Technique for Reference Tracking Under Shot Noise

Eda Erol[1,*] and Mustafa Dogru[1,*] and Ismail Uyanık[1]

***Abstract*— Sensor fusion enhances robotic perception by integrating data from multiple sensing modalities. This paper introduces a biologically inspired, closed-loop sensor fusion framework combining camera and LiDAR data to robustly estimate the position of a moving object. To mitigate non-Gaussian disturbances such as shot noise, the approach employs dynamic weighting strategies integrated with the Maximum Correntropy Criterion Kalman Filter (MCC-KF). The proposed method is validated experimentally using a custom-built platform, demonstrating enhanced robustness and accuracy under diverse and challenging noise conditions.**

KEYWORDS

Kalman filter, sensor fusion, shot noise, MCC-KF, robotics, adaptive weighting.

I. INTRODUCTION

Sensor fusion plays a crucial role in modern intelligent systems by integrating measurements from multiple sensors, thus improving perceptual accuracy and robustness [1]–[3]. Applications of sensor fusion are widespread, spanning autonomous vehicles, medical robotics, surveillance, and industrial automation [4], [5].

However, sensor measurements in real-world environments often experience non-Gaussian disturbances such as shot noise, abrupt outliers, and transient faults, significantly degrading the performance of traditional fusion methods reliant on Gaussian assumptions [6]. Specifically, conventional Kalman filters, optimal under linear and Gaussian conditions, exhibit vulnerabilities to heavy-tailed noise distributions and sudden measurement anomalies.

To address these limitations, we propose an adaptive sensor fusion framework combining vision and LiDAR measurements for real-time target tracking under variable and non-Gaussian noise conditions. Our approach leverages the Maximum Correntropy Criterion Kalman Filter (MCC-KF) [6], which substitutes the traditional mean-square-error cost function with a correntropy-based criterion, inherently robust against impulsive disturbances. Furthermore, we enhance estimator adaptability by dynamically adjusting the measurement noise covariance through residual-based adaptation techniques, namely Moving Window (MW) and Forgetting Factor (FF) strategies [7]–[9].

This paper contributes to the field in multiple ways. First, we develop a real-time, closed-loop sensor fusion platform integrating a camera (Logitech) and a LiDAR (Hokuyo) sensor, validated through both simulation and experiments on a custom-built setup. Second, we systematically evaluate four sensor fusion techniques—static weighted averaging, classical Kalman Filtering, MCC-KF, and MCC-KF with residual-based adaptation—under varying noise conditions, including controlled shot noise injection. Lastly, we introduce a hybrid adaptive fusion scheme that jointly optimizes the Kalman gain and updates noise covariance estimates, significantly enhancing resilience to non-Gaussian disturbances.

Recent studies have explored robust filtering under non-Gaussian noise using MCC-based techniques, such as MCC filtering for wireless sensor networks [6] and adaptive gain tuning for fault-tolerant tracking [7]. However, these approaches often focus on simulation-based validation without real-time closed-loop implementation. In contrast, our approach integrates MCC-KF with dynamic noise modeling into a physically validated robotic tracking platform, demonstrating superior robustness to shot noise and sensor degradation in practical environments.

II. SYSTEM MODEL

The robotic tracking system is modeled as a multisensory closed-loop control architecture, as illustrated in Figure 1. Two independent sensing modalities—camera and LiDAR—simultaneously observe the same target. The system estimates the true target position by fusing these measurements and subsequently drives an actuator to track the estimated position [10], [11].

Let $Y(s)$ represent the Laplace transform of the actuator platform's output position. The desired target positions detected by the camera and LiDAR are denoted by $R_V(s)$ and $R_L(s)$, respectively. A Proportional-Integral (PI) controller, $C(s)$, acts on the tracking error to regulate the actuator dynamics, represented by the transfer function $P(s)$.

Sensor fusion is realized through dynamic weighting functions $V(s)$ and $L(s)$, which reflect the reliability (confidence level) of the camera and LiDAR measurements, respectively. The control law is defined as a weighted sum of sensor errors:

$$Y(s) = [(R_V(s) - Y(s))V(s) + (R_L(s) - Y(s))L(s)]\, C(s)P(s). \quad (1)$$

This equation illustrates how individual sensor tracking errors are dynamically weighted and combined to generate the actuation signal. The closed-loop system dynamics can be simplified to the following transfer function:

[1]Eda Erol , Mustafa Dogru and Ismail Uyanik are with the Department of Electrical and Electronics Engineering, Hacettepe University, 06800 Ankara, Türkiye eda.erol@turktelekom.com.tr, mustafa.y@hacettepe.edu.tr, uyanik@ee.hacettepe.edu.tr

[*]Authors contributed equally.

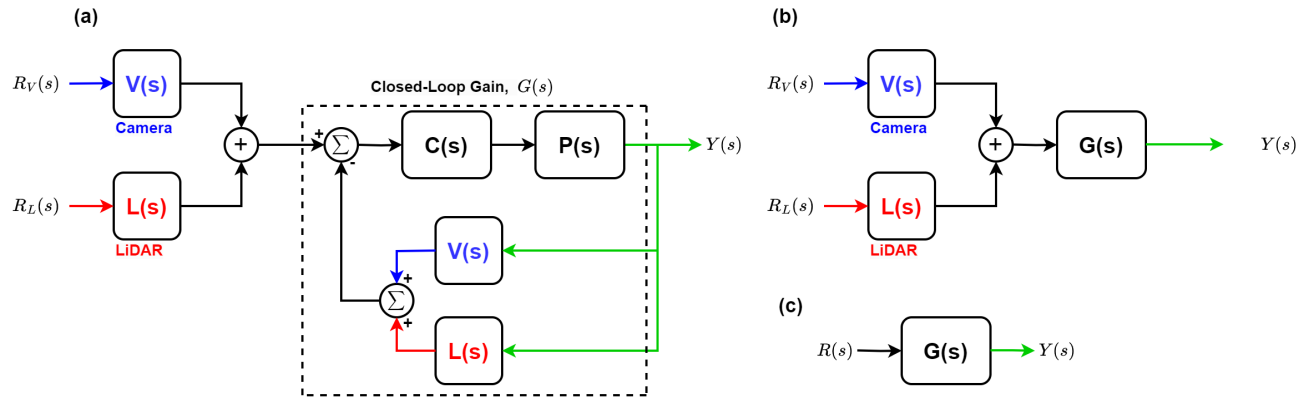

Fig. 1: Block diagram of the multisensory closed-loop tracking system. The system consists of reference signals from the camera $R_V(s)$ and LiDAR $R_L(s)$, which are compared with the actuator output $Y(s)$ to form error signals. These errors are scaled by reliability weights $V(s)$ and $L(s)$, then combined and passed through the controller $C(s)$ and plant $P(s)$ to generate the actuation command.

$$G(s) = \frac{C(s)P(s)}{1 + C(s)P(s)(V(s) + L(s))}. \tag{2}$$

This formulation reveals that closed-loop bandwidth and stability are influenced not only by controller and plant dynamics but also by the fusion weights. Dynamically adjusting $V(s)$ and $L(s)$ enables the system to prioritize more reliable sensor inputs in real-time [12].

The discrete-time state-space representation employed in Kalman filtering uses the following state vector:

$$\mathbf{x}_k = \begin{bmatrix} x_{\text{LiDAR}}(k) \\ v_{\text{LiDAR}}(k) \\ x_{\text{Camera}}(k) \\ v_{\text{Camera}}(k) \end{bmatrix}, \tag{3}$$

which encapsulates position and velocity information for each sensor modality. Position measurements are directly obtained from LiDAR and camera data, while velocities are inferred from differences between consecutive measurements.

The process noise covariance matrix Q captures modeling errors and uncertainties associated with system acceleration. It is derived from the acceleration noise variance σ_a^2 based on a constant acceleration model discretized over time interval Δt:

$$Q = \sigma_a^2 \begin{bmatrix} \frac{\Delta t^4}{4} & \frac{\Delta t^3}{2} & 0 & 0 \\ \frac{\Delta t^3}{2} & \Delta t^2 & 0 & 0 \\ 0 & 0 & \frac{\Delta t^4}{4} & \frac{\Delta t^3}{2} \\ 0 & 0 & \frac{\Delta t^3}{2} & \Delta t^2 \end{bmatrix}. \tag{4}$$

This matrix quantifies uncertainty in position and velocity predictions resulting from acceleration variations and serves as a foundation for predicting error covariance within the Kalman filter framework.

III. Experimental Setup

The experimental platform was carefully designed and constructed to facilitate real-time, repeatable evaluation of sensor fusion algorithms under controlled laboratory conditions, as illustrated in Figure 2. The setup comprises three precision linear stages, each serving a specific purpose within a closed-loop tracking system influenced by different sensory feedback modalities:

- The first stage supports the sensing module, consisting of a monocular camera and a 2D LiDAR unit mounted on a rigid frame. This stage emulates the mobile sensing platform.
- The second stage holds a visual tracking target explicitly designed for reliable detection via frame-by-frame image processing.
- The third stage contains a planar target featuring high reflectivity and distinct geometric characteristics optimized for LiDAR-based tracking.

All axes are driven by digitally actuated linear motion modules capable of executing precisely timed trajectories. A dedicated embedded controller synchronizes motor commands and facilitates real-time communication with the host

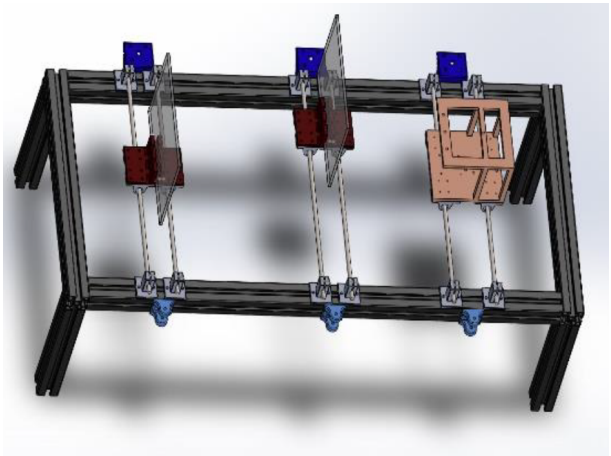

Fig. 2: Comprehensive layout of the experimental platform including sensor stage, target stages.

system. An isolated supply architecture ensures stable power distribution and maintains signal integrity.

A modular software stack built upon the Robot Operating System (ROS) ensures deterministic operation of the sensor fusion pipeline. Visual data are processed using morphological operations and geometric centroiding implemented in OpenCV, while LiDAR returns are filtered and thresholded to isolate prominent planar features.

All sensor streams are timestamp-aligned, transformed into a unified reference frame, and pre-filtered prior to entering the fusion algorithms. Control commands, derived from the fused position estimates, are transmitted to motion controllers in a closed-loop arrangement, thus completing the sensory-actuation feedback loop.

This experimental setup not only facilitates validation of Kalman-based estimation methods but also allows systematic injection of Gaussian and non-Gaussian disturbances. Consequently, the platform enables robust performance analysis under diverse environmental conditions [10].

A. Sensor Data Preprocessing

Robust target localization is achieved through separate preprocessing pipelines for camera and LiDAR data.

For the camera, visual tracking is performed using two circular markers—one attached to the moving target and another serving as a static world reference. Each frame is converted to grayscale, binarized using adaptive thresholding, and the centroids of the two markers are extracted using geometric moment analysis. The relative distance between these centroids defines the perceived displacement of the target.

For the LiDAR, only points falling within a predefined angular sector and range window are retained. Spurious reflections and background clutter are removed using outlier suppression techniques. The position of the target is computed by determining the median distance of the filtered return points, which minimizes the influence of noise and provides robust center localization.

B. ROS Architecture

The system employs a modular ROS-based architecture with individual sensor nodes continuously publishing raw and processed position measurements to a central fusion node. This fusion node applies the chosen algorithm—weighted average, Kalman Filter, or MCC-KF—and outputs the fused estimate.

A dedicated control node calculates control signals from the fused position estimate, forwarding commands to the motor controller via real-time serial communication. The pipeline operates at a consistent update rate, synchronized using ROS timers and timestamps, ensuring stable, low-latency closed-loop feedback.

IV. Proposed Method

This section presents a systematic progression of sensor fusion techniques, arranged by increasing robustness and complexity. All methods are evaluated within the experimental framework previously described.

A. Weighted Average Fusion

The simplest fusion approach is based on the Minimum Variance Unbiased Estimator (MVUE). Assume two noisy observations of the same physical variable x: $s_1 = x + v_1$ and $s_2 = x + v_2$, where v_1 and v_2 are independent, zero-mean Gaussian noise components with known variances σ_1^2 and σ_2^2. The fused estimate $\hat{x}$ is computed using a linear weighted combination:

$$\hat{x} = w_1 s_1 + w_2 s_2, \quad \text{where} \quad w_1 + w_2 = 1 \tag{5}$$

The optimal weights that minimize the mean squared error (MSE) are derived as:

$$w_1 = \frac{\sigma_2^2}{\sigma_1^2 + \sigma_2^2}, \qquad w_2 = \frac{\sigma_1^2}{\sigma_1^2 + \sigma_2^2} \tag{6}$$

This method is optimal only under the assumption of stationary and Gaussian noise, and lacks the ability to adapt in real time to changing noise characteristics [10].

B. Kalman Filter with Constant Velocity Model

To incorporate motion dynamics, we model the system as a linear discrete-time state-space model under the constant velocity assumption:

$$\mathbf{x}_{k+1} = A\mathbf{x}_k + \mathbf{w}_k \tag{7}$$

$$\mathbf{y}_k = C\mathbf{x}_k + \mathbf{v}_k \tag{8}$$

where $\mathbf{x}_k$ is the state vector, $\mathbf{w}_k$ is the process noise (zero-mean with covariance Q), and $\mathbf{v}_k$ is the measurement noise (zero-mean with covariance R) [6]. The state vector includes both position and velocity from each sensor channel:

$$\mathbf{x}_k = [x_{\text{LiDAR}}(k),\ v_{\text{LiDAR}}(k),\ x_{\text{Camera}}(k),\ v_{\text{Camera}}(k)]^T \tag{9}$$

The system matrices are defined as follows: $A \in \mathbb{R}^{d_x \times d_x}$, $\mathbf{w}_k \sim \mathcal{N}(\mathbf{w}_k; \mathbf{0}, Q)$ where $Q \geq 0 \in \mathbb{R}^{d_x \times d_x}$ is the process noise covariance; $C \in \mathbb{R}^{d_y \times d_x}$, $\mathbf{v}_k \sim \mathcal{N}(\mathbf{v}_k; \mathbf{0}, R)$ where $R \geq 0 \in \mathbb{R}^{d_y \times d_y}$ is the measurement noise covariance. The recursive Kalman Filter consists of two phases:

- **Prediction:**

$$\hat{\mathbf{x}}_{k|k-1} = A\hat{\mathbf{x}}_{k-1|k-1} \tag{10}$$

$$P_{k|k-1} = AP_{k-1|k-1}A^T + Q \tag{11}$$

- **Update:**

$$K_k = P_{k|k-1}C^T(CP_{k|k-1}C^T + R)^{-1} \tag{12}$$

$$\hat{\mathbf{x}}_{k|k} = \hat{\mathbf{x}}_{k|k-1} + K_k(\mathbf{y}_k - C\hat{\mathbf{x}}_{k|k-1}) \tag{13}$$

$$P_{k|k} = (I - K_k C)P_{k|k-1} \tag{14}$$

C. Residual-Based Adaptive Kalman Filter

In realistic environments, the measurement noise statistics may vary due to lighting conditions, occlusions, or sensor degradation [11], [13]. To address this, we estimate the measurement noise covariance R_k online using innovation-based residuals:

$$\epsilon_k = \mathbf{y}_k - C\hat{\mathbf{x}}_{k|k-1} \tag{15}$$

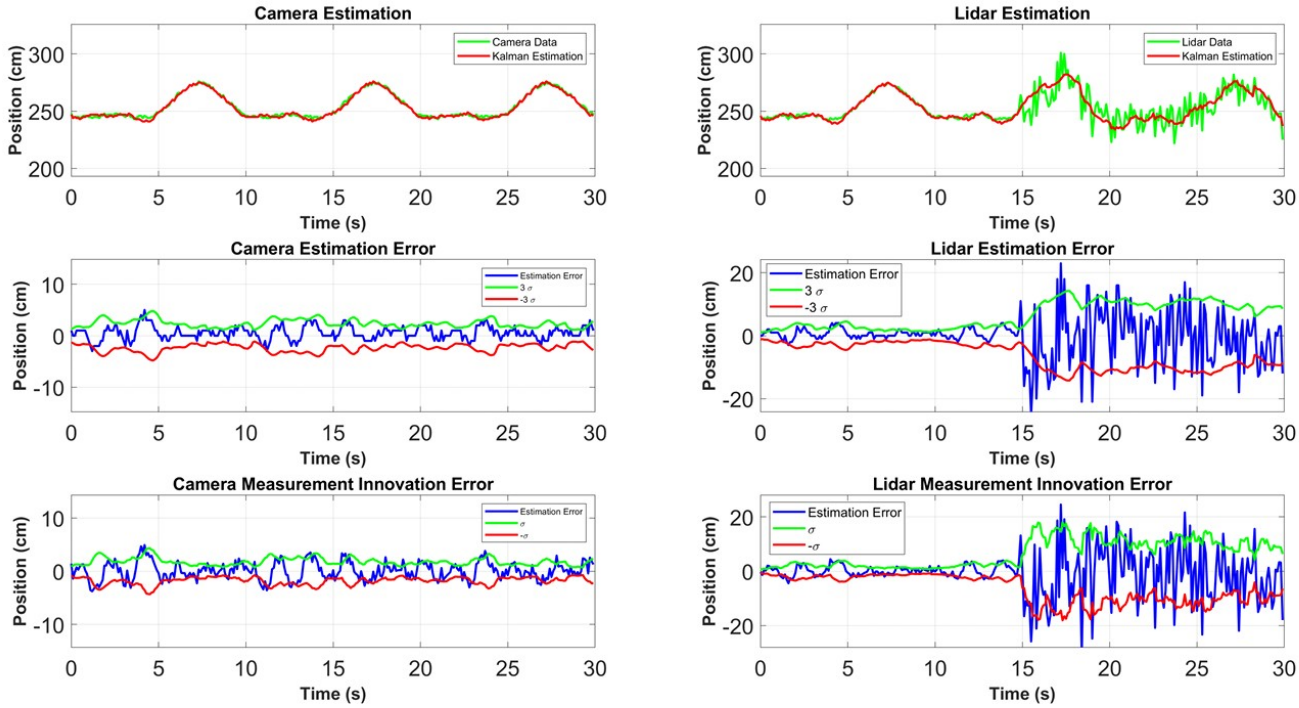

Fig. 3: Performance of full method under shot noise and variable sensor reliability.

Two techniques are used:

- **Moving Window (MW):**

$$\hat{R}_k = \frac{1}{N} \sum_{i=k-N+1}^{k} \epsilon_i \epsilon_i^T + C P_k C^T \tag{16}$$

- **Forgetting Factor (FF):**

$$\hat{R}_k = \alpha \hat{R}_{k-1} + (1-\alpha)(\epsilon_k \epsilon_k^T + C P_k C^T) \tag{17}$$

These methods allow the Kalman filter to track non-stationary noise profiles in real time [7].

D. Maximum Correntropy Criterion Kalman Filter (MCC-KF)

The MCC-KF improves robustness to outliers by replacing the MSE cost function with one based on correntropy, which measures similarity in a high-dimensional kernel space [6], [14]. The cost function is:

$$J_m = \exp\left(-\frac{\|\mathbf{y}_k - C\hat{\mathbf{x}}_k\|^2_{R_k^{-1}}}{2z^2}\right) + \exp\left(-\frac{\|\hat{\mathbf{x}}_k - A\hat{\mathbf{x}}_{k-1}\|^2_{P_{k|k-1}^{-1}}}{2z^2}\right) \tag{18}$$

Here, z is the kernel width parameter controlling sensitivity to outliers. The gain is scaled by a factor:

$$L_k = \frac{\exp\left(-\frac{\|\mathbf{y}_k - C\hat{\mathbf{x}}_k\|^2_{R_k^{-1}}}{2z^2}\right)}{\exp\left(-\frac{\|\hat{\mathbf{x}}_k - A\hat{\mathbf{x}}_{k-1}\|^2_{P_{k|k-1}^{-1}}}{2z^2}\right)} \tag{19}$$

leading to the modified Kalman gain:

$$K_k = \left(P_{k|k-1}^{-1} + L_k C^T R_k^{-1} C\right)^{-1} L_k C^T R_k^{-1} \tag{20}$$

E. MCC-KF with Adaptive Noise Estimation

The most robust strategy combines MCC-KF with dynamic R_k estimation [7]. The algorithm proceeds as follows:

- Predict $\hat{\mathbf{x}}_{k|k-1}$ and $P_{k|k-1}$
- Update R_k using MW or FF
- Compute L_k from residuals
- Compute gain K_k using correntropy cost
- Update $\hat{\mathbf{x}}_{k|k}$ and $P_{k|k}$

This hybrid approach enables the filter to suppress outliers while adapting to changing noise statistics, making it highly suitable for real-time robotics applications under variable conditions [6]–[8]. The resulting performance is visualized in Figure 3.

V. Results and Discussion

This section presents a comparative evaluation of the proposed sensor fusion methods under three controlled noise scenarios. The RMSE values for different methods across scenarios are shown in Figure 5. Both quantitative and qualitative analyses are provided. The primary quantitative metric is Root Mean Square Error (RMSE) between estimated and ground-truth positions. In addition, spectral analysis using the Fast Fourier Transform (FFT) is included to assess noise attenuation performance in the frequency domain. Tracking plots further illustrate the real-time behavior of each algorithm.

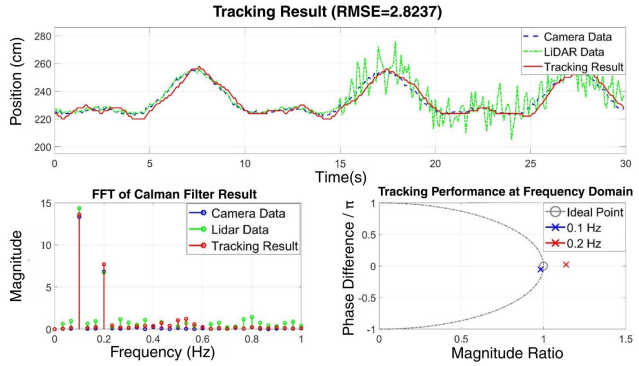

Fig. 4

Fig. 5: Frequency Domain Comparison using FFT: High-frequency suppression performance of each method.

A. Scenario I: Baseline with Low Noise

Under minimal environmental noise, all fusion methods perform satisfactorily. Weighted average fusion yields acceptable results due to consistent sensor variances [7]. The standard Kalman Filter improves accuracy further by leveraging system dynamics [6]. The MCC-KF method performs similarly to the classical KF in this setting, as there are no significant outliers to exploit the strength of the correntropy-based formulation [6].

B. Scenario II: Gaussian Noise Injection

To simulate challenging but common real-world noise conditions, additive Gaussian noise is introduced into the visual sensor data [15], [16]. Under these conditions, the static weighted average method suffers due to its inability to adapt [10]. The Kalman Filter achieves better accuracy but remains limited by its assumption of stationary noise covariance [6].

The residual-based adaptive Kalman Filters—Moving Window (MW) and Forgetting Factor (FF)—significantly enhance the system's robustness [7], [11]. By updating the measurement noise covariance R_k in real-time, they allow the estimator to better match the observed uncertainty. Among them, the FF-based filter provides a good balance between responsiveness and stability [11].

C. Scenario III: Shot Noise and Outlier Bursts

To emulate sudden, non-Gaussian disturbances such as lighting flicker or sensor misreads, shot noise is periodically injected [6]. In this case:

- The Kalman Filter without adaptation shows notable performance degradation [11].
- MCC-KF demonstrates clear superiority by suppressing the influence of outliers through its correntropy-based gain modification [6], [14].
- The MCC-KF combined with residual-based noise adaptation (MW or FF) achieves the highest accuracy and stability under bursty noise [7].

D. Spectral Analysis via FFT

To further evaluate noise attenuation performance, frequency-domain characteristics of the estimated position signals are analyzed using FFT [15]. As shown in Figure 6, the proposed hybrid MCC-KF method exhibits the lowest spectral energy in the high-frequency bands, indicating superior suppression of transient and impulsive disturbances compared to other methods.

E. Qualitative Evaluation

In addition to RMSE and FFT metrics, trajectory plots further illustrate the tracking accuracy of each method. The proposed hybrid MCC-KF method exhibits minimal tracking delay and negligible overshoot during transient disturbances [6], [7]. Its output trajectory closely follows the true path, even under bursty shot noise conditions, as shown in Figure 7.

VI. Conclusion

This paper presented a biologically inspired, robust sensor fusion framework tailored for real-time target tracking under variable and non-Gaussian noise conditions. Starting from basic weighted average fusion [7], we progressively integrated classical Kalman filtering [6], residual-based noise adaptation [11], and ultimately the Maximum Correntropy Criterion Kalman Filter (MCC-KF) [4], [6], [14] to handle bursty outliers.

The final hybrid method, which combines MCC-KF with residual-based dynamic noise estimation, demonstrated superior accuracy, low RMSE, and high resilience under challenging experimental conditions including injected shot noise [7]. These results were consistently observed across both quantitative [12], [15] and qualitative evaluations [4].

All methodologies were implemented and validated on a closed-loop experimental testbed [10], ensuring reproducibility and real-world applicability. The system's performance illustrates the efficacy of incorporating biologically inspired noise handling strategies [17], [18] within adaptive estimation frameworks [11], [19]–[21].

Future research directions include extending the architecture to multi-dimensional tracking scenarios, optimizing computational efficiency for embedded platforms [5], and integrating the fusion system with SLAM algorithms for autonomous robotic navigation [22].

ACKNOWLEDGMENT

This work was supported by the Scientific and Technological Research Council of Turkiye (TÜBİTAK) under Grant No. 122E464 and Hacettepe University Scientific Projects Unit under Grant No. 20240 awarded to Dr. Ismail Uyanik. This work of Eda Erol is supported by TÜBİTAK 1515 Frontier R&D Laboratories Support Program for Turk Telekom neXt Generation Technologies Lab (XGeNTT) under project number 5249902.

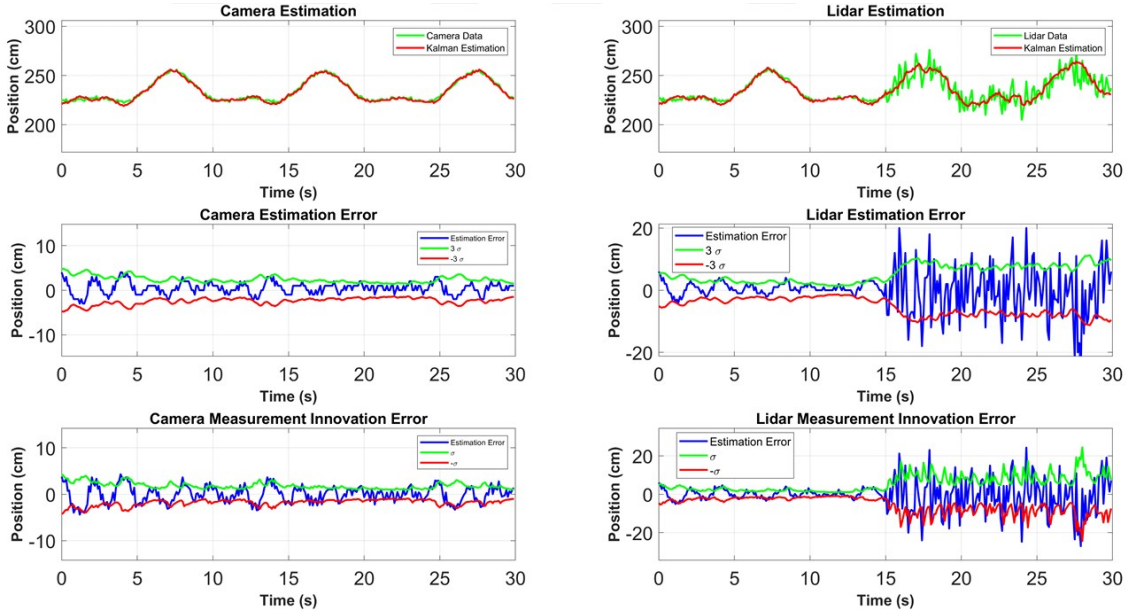

Fig. 6: RMSE Comparison for All Methods Across Noise Scenarios

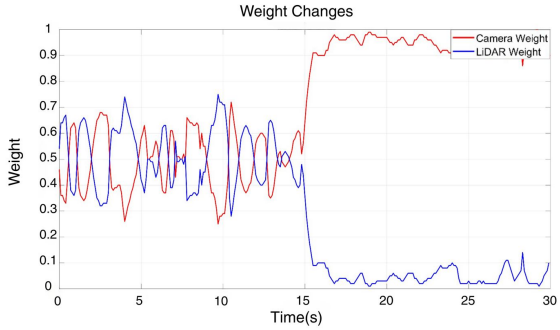

Fig. 7: Comparison of Tracking Accuracy under Shot Noise

REFERENCES

[1] D. L. Hall and J. Llinas, "An introduction to multisensor data fusion," *Proceedings of the IEEE*, vol. 85, no. 1, pp. 6–23, 1997.

[2] R. Luo and M. Kay, "Multisensor integration and fusion in intelligent systems," *IEEE Transactions on Systems, Man, and Cybernetics*, vol. 19, no. 5, pp. 901–931, 1989.

[3] J. Drugowitsch, G. C. DeAngelis, E. M. Klier, D. E. Angelaki, and A. Pouget, "Optimal multisensory decision-making in a reaction-time task," *Elife*, vol. 3, 2014.

[4] J. Kocić, N. Jovičić, and V. Drndarević, "Sensors and sensor fusion in autonomous vehicles," in *2018 26th Telecommunications Forum (TELFOR)*, pp. 420–425, 2018.

[5] D. Singh, G. Tripathi, and A. J. Jara, "A survey of internet-of-things: Future vision, architecture, challenges and services," in *2014 IEEE World Forum on Internet of Things (WF-IoT)*, pp. 287–292, 2014.

[6] R. Gurajala, P. B. Choppala, J. S. Meka, and P. D. Teal, "Derivation of the kalman filter in a bayesian filtering perspective," in *2021 2nd International Conference on Range Technology*, pp. 1–5, 2021.

[7] V. G. Voinov and M. S. Nikulin, *Unbiased estimators and their applications: volume 1: univariate case*, vol. 263. Springer Science & Business Media, 2012.

[8] H. R. Patel and V. A. Shah, "Comparative analysis between two fuzzy variants of harmonic search algorithm: Fuzzy fault tolerant control application," *IFAC-PapersOnLine*, vol. 55, no. 7, pp. 507–512, 2022.

[9] H. R. Patel and V. A. Shah, "General type-2 fuzzy logic systems using shadowed sets: a new paradigm towards fault-tolerant control," in *2021 Australian & New Zealand Control Conference*, pp. 116–121, 2021.

[10] R. Luo and M. Kay, "A tutorial on multisensor integration and fusion," in *[Proceedings] IECON '90: 16th Annual Conference of IEEE Industrial Electronics Society*, pp. 707–722 vol.1, 1990.

[11] R. C. Luo, C.-C. Yih, and K. L. Su, "Multisensor fusion and integration: approaches, applications, and future research directions," *IEEE Sensors journal*, vol. 2, no. 2, pp. 107–119, 2002.

[12] D. Smith and S. Singh, "Approaches to multisensor data fusion in target tracking: A survey," *IEEE transactions on knowledge and data engineering*, vol. 18, no. 12, pp. 1696–1710, 2006.

[13] I. Uyanik, S. A. Stamper, N. J. Cowan, and E. S. Fortune, "Sensory cues modulate smooth pursuit and active sensing movements," *Frontiers in behavioral neuroscience*, vol. 13, p. 59, 2019.

[14] S. P. Windsor, R. J. Bomphrey, and G. K. Taylor, "Vision-based flight control in the hawkmoth hyles lineata," *Journal of The Royal Society Interface*, vol. 11, no. 91, 2014.

[15] M. L. Fung, M. Z. Q. Chen, and Y. H. Chen, "Sensor fusion: A review of methods and applications," in *2017 29th Chinese Control And Decision Conference (CCDC)*, pp. 3853–3860, 2017.

[16] J. Hirokawa, O. Sadakane, S. Sakata, M. Bosch, Y. Sakurai, and T. Yamamori, "Multisensory information facilitates reaction speed by enlarging activity difference between superior colliculus hemispheres in rats," *PloS one*, vol. 6, no. 9, 2011.

[17] E. E. Sutton, A. Demir, S. A. Stamper, E. S. Fortune, and N. J. Cowan, "Dynamic modulation of visual and electrosensory gains for locomotor control," *Journal of The Royal Society Interface*, vol. 13, no. 118, 2016.

[18] N. J. Cowan, M. M. Ankarali, J. P. Dyhr, M. S. Madhav, E. Roth, S. Sefati, S. Sponberg, S. A. Stamper, E. S. Fortune, and T. L. Daniel, "Feedback control as a framework for understanding tradeoffs in biology," *American Zoologist*, vol. 54, no. 2, pp. 223–237, 2014.

[19] M. A. Frye and M. H. Dickinson, "Motor output reflects the linear superposition of visual and olfactory inputs in drosophila," *Journal of Experimental Biology*, vol. 207, no. 1, pp. 123–131, 2004.

[20] I. Uyanik, S. Sefati, S. A. Stamper, K.-A. Cho, M. M. Ankarali, E. S. Fortune, and N. J. Cowan, "Variability in locomotor dynamics reveals the critical role of feedback in task control," *Elife*, vol. 9, 2020.

[21] M. S. Comertler and I. Uyanik, "Salience of multisensory feedback regulates behavioral variability," *Bioinspiration & Biomimetics*, vol. 17, no. 1, 2021.

[22] A. Yilmaz, "Sensor fusion in computer vision," in *2007 Urban Remote Sensing Joint Event*, pp. 1–5, Institute of Electrical and Electronics Engineers, 2007.